

## Electromagnetic properties of manganese-zinc ferrite with lithium substitution

E. De Fazio<sup>a</sup>, P. G. Bercoff<sup>b\*</sup> and S. E. Jacobo<sup>a</sup>

<sup>a</sup>LAFMACEL, Facultad de Ingeniería, Universidad de Buenos Aires. Paseo Colón 850 (1063), Buenos Aires, Argentina.

<sup>b</sup>FAMAF, Universidad Nacional de Córdoba. IFEG-Conicet. Ciudad Universitaria (5000) Córdoba, Argentina.

\*corresponding author. E-mail: bercoff@famaf.unc.edu.ar. Tel.: +54 351 433 4051 extension 103. Fax: +54 351 433 4054.

**Keywords:** MnZn ferrites, magnetic nanoparticles, lithium substitution, EM-wave absorbers

**Abstract.** Polycrystalline manganese-zinc ferrite with lithium substitution of composition  $\text{Li}_{0.5x}\text{Mn}_{0.4}\text{Zn}_{0.6-x}\text{Fe}_{2+0.5x}\text{O}_4$  ( $0.0 \leq x \leq 0.4$ ) were prepared by the usual ceramic method. X-ray diffraction analysis confirmed that the samples have a spinel structure and are single-phase for some values of Li content. Lithium doping considerably modifies saturation magnetization since its value increases from 57.5 emu/g for  $x=0.0$  to 82.9 emu/g for  $x=0.4$ . Lithium inclusion increases the real permeability (over 1MHz) while the natural resonance frequency shifts to lower values as the fraction of Li increases. These ferrites show good electromagnetic properties as absorbers in the microwave range of 1MHz-1GHz.

### 1. Introduction

Polycrystalline ferrites have been extensively used in many electronic devices because of their high permeability in the radio frequency region, high electrical resistivity, mechanical strength and chemical stability. Their electrical properties are dependent on several factors such as the preparation method, substitution with different cations and grain structure or size. In particular, Mn-Zn ferrites are very important soft magnetic materials because of their high initial magnetic permeability, saturation magnetization and electrical resistivity [1-4].

Due to their low power losses, they are particularly useful in electromagnetic components like rotary transformers, deflection yoke cores and intermediate frequency transformer cores. Li and Li-substituted ferrites have been found to be excellent materials in high density recording media and absorbers and microwave devices due to their low cost, high saturation magnetization, high Curie temperature and hysteresis loop properties, which offer advantageous performances over other spinel structures [1-6]. However, no reports have been found in the literature on microwave properties of Li-substituted Mn-Zn ferrites. In the present work, the influence of lithium substitution on structural, magnetic and dielectric properties of  $\text{Li}_{0.5x}\text{Mn}_{0.4}\text{Zn}_{0.6-x}\text{Fe}_{2+0.5x}\text{O}_4$  ( $0.0 \leq x \leq 0.4$ ), prepared by the ceramic method, is presented. Furthermore, it is shown that it is possible to design a single-layered electromagnetic wave absorber with good properties by using polycrystalline Li-Mn-Zn ferrite.

### 2. Experimental

Analytical grade  $\text{Li}_2\text{CO}_3$ , ZnO,  $\text{Fe}_2\text{O}_3$  and  $\text{MnSO}_4 \cdot 5\text{H}_2\text{O}$  were used to prepare Li-Zn-Mn ferrites by the usual ceramic method [7,8]. Samples with overall composition  $\text{Li}_{0.5x}\text{Mn}_{0.4}\text{Zn}_{0.6-x}\text{Fe}_{2+0.5x}\text{O}_4$  ( $0.0 \leq x \leq 0.4$ ) were prepared by mixing the powders with the stoichiometric ratio. The final mixture was calcined at 1100 °C for two hours in nitrogen flow. The samples were structurally characterized by X-ray diffraction with a Philips diffractometer using Cu K $\alpha$  radiation. Crystallite sizes were calculated from the FWHM of the (311) reflection using the Scherrer formula corrected for instrumental broadening. Cell parameters were calculated from X-ray patterns using the program Powder Cell. The morphology of the powder samples was examined by scanning electron

microscopy (SEM) with a Zeiss DSM 982 GEMINI. Magnetic measurements were performed at room temperature using a LakeShore 7300 vibrating sample magnetometer with maximum applied field of 15 kOe. Complex permeability ( $\mu' + i\mu''$ ) of toroids and complex permittivity ( $\epsilon' + i\epsilon''$ ) of pellets were measured on a HP4291A Material Analyser from 1 to 1800 MHz.

### 3. Results and Discussion

Figure 1 shows the diffraction patterns of the series  $\text{Li}_{0.5x}\text{Mn}_{0.4}\text{Zn}_{0.6-x}\text{Fe}_{2+0.5x}\text{O}_4$ , for  $x=0.0$  to  $0.4$ . No secondary phases are detected for  $x=0, 0.1, 0.3$  and  $0.4$  –the observed peaks correspond only to the spinel phase. Surprisingly, for  $x=0.2$  weak signals of secondary phases (5%) are present. These peaks are indexed as the precursor oxides ( $\text{Fe}_2\text{O}_3$  and  $\text{ZnO}$ ) indicating that the reaction was not completed in this sample. A monotonous displacement of the peaks position to higher angles is observed (shown in the inset of Figure 1 for the (511) reflection) indicating a decrease in the cell parameter. This was confirmed after refining the spectra, obtaining cell parameters that range from  $8.546(1)$  Å for  $x=0.0$  to  $8.412(1)$  Å for  $x=0.4$  (Table 1). The observed decrease in the lattice parameter with increasing substitution can be explained on the basis of the relative ionic radii. As the ionic radius of  $\text{Li}^+$  ions ( $0.78$  Å) and  $\text{Fe}^{3+}$  ions ( $0.67$  Å) are smaller than the ionic radius of  $\text{Zn}^{2+}$  ( $0.82$  Å), the lithium and extra iron incorporated in both the tetrahedral and octahedral sites cause the decrease in the lattice constant [9].

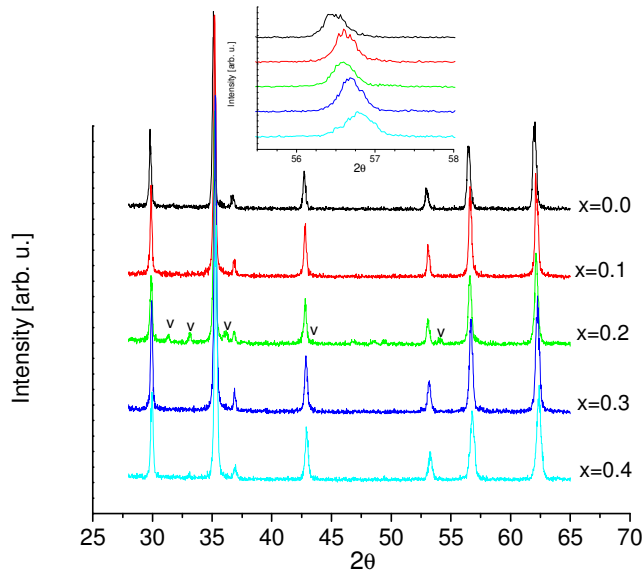


**Figure 1.** X-ray diffraction patterns of the series  $\text{Li}_{0.5x}\text{Mn}_{0.4}\text{Zn}_{0.6-x}\text{Fe}_{2+0.5x}\text{O}_4$ , for  $x=0.0$  to  $0.4$ . All the peaks correspond to reflections of the spinel phase, except for those marked with a v, which correspond to the precursors  $\text{Fe}_2\text{O}_3$  and  $\text{ZnO}$ . The inset shows a slight displacement to higher angle which occurs for all the peaks.

SEM images of the calcined powders at  $1100^\circ\text{C}$  for 2 hours are shown in Figures 2a-2e for the different  $x$  values. Samples are agglomerated and show polyhedral shapes. It was found that the average grain size estimated from the geometric analysis is approximately  $1\ \mu\text{m}$  and is almost independent of the Li content,  $x$ .

Table 1: Cell parameter  $a$ , crystallite size  $d$  and saturation magnetization  $M_s$  for the set of studied samples.

Li content (x)	Cell parameter $a$ [ $\pm 0.001\text{\AA}$ ]	Crystallite size $D$ [ $\pm 5$ nm]	$M_s$ [emu/g]
0.0	8.546	55	57.5
0.1	8.437	54	79.5
0.2	8.442	50	78.9
0.3	8.429	68	81.3
0.4	8.412	65	82.9

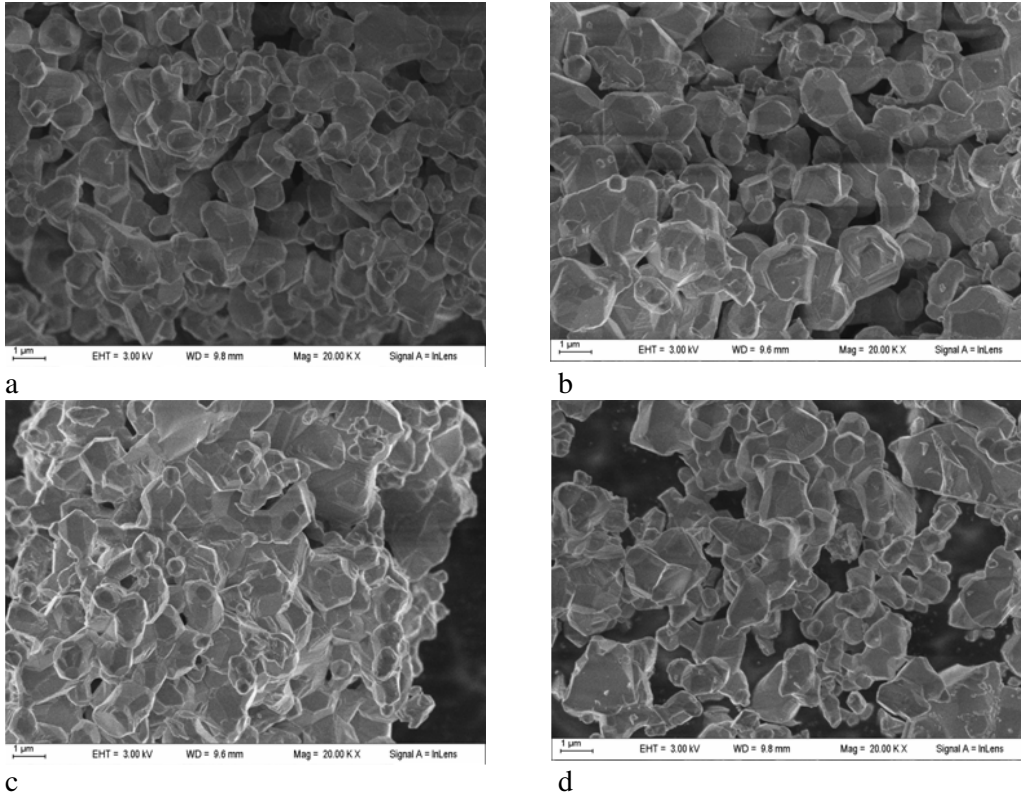


**Figure 2.** SEM images of  $\text{Li}_{0.5x}\text{Mn}_{0.4}\text{Zn}_{0.6-x}\text{Fe}_{2+0.5x}\text{O}_4$  for different values of  $x$ : 0.0 (a), 0.1 (b), 0.2 (c), 0.3 (d) and 0.4 (e).

Saturation magnetization  $M_s$  as a function of Li content of the series  $\text{Li}_{0.5x}\text{Mn}_{0.4}\text{Zn}_{0.6-x}\text{Fe}_{2+0.5x}\text{O}_4$  is shown in Figure 3. All the samples saturate at fields below 15 kOe. Li doping considerably modifies  $M_s$  since its value increases from 57.5 emu/g for  $x=0.0$  to 82.9 emu/g for  $x=0.4$  (see Table 1 and Figure 3). The inclusion of  $\text{Li}^+$  and extra  $\text{Fe}^{3+}$  in the lattice promotes a cation arrangement between tetrahedral and octahedral sites that increases  $M_s$  to rather high values. The low value for  $x=0.2$  can be related to the presence of a secondary phase (see Figure 1).

Coercivity is low in every case, with values around and below 10 Oe. Such a soft behavior has already been reported for MnZn ferrites [10].

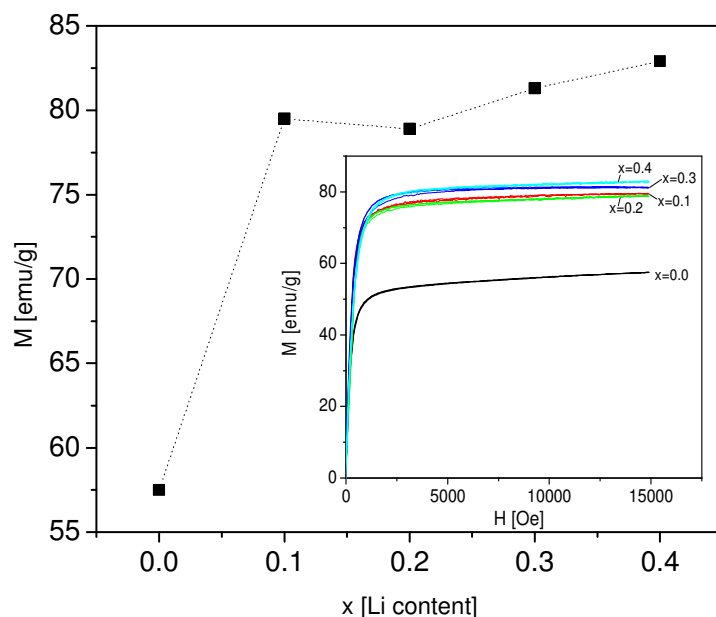


**Figure 3.** Saturation magnetization as a function of Li content for the series  $\text{Li}_{0.5x}\text{Mn}_{0.4}\text{Zn}_{0.6-x}\text{Fe}_{2+0.5x}\text{O}_4$ . The inset shows the first quadrant of the corresponding hysteresis loops.

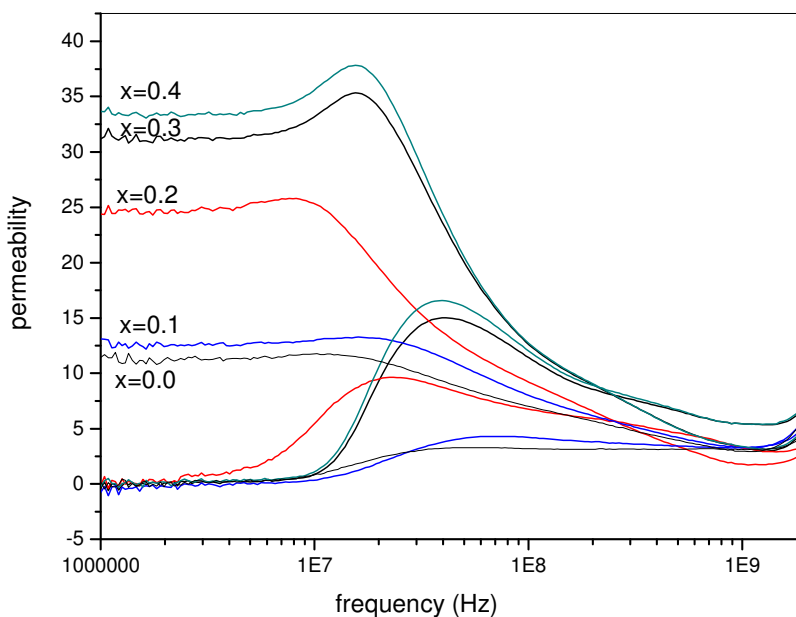


**Figure 4.** Real and imaginary permeability of  $\text{Li}_{0.5x}\text{Mn}_{0.4}\text{Zn}_{0.6-x}\text{Fe}_{2+0.5x}\text{O}_4$  in the 1MHz-1.8GHz range.

The complex relative permeability spectra of the studied ferrites are shown in Figure 4. The real part of the permeability ( $\mu'$ ) remains almost constant until the frequency is raised up to a certain value, and then decreases at higher frequency. The imaginary permeability ( $\mu''$ ) gradually increases with the frequency, and presents a broad maximum at a certain frequency, where the real permeability rapidly decreases. This feature is well known as the natural resonance. It is found that

the real permeability in the low-frequency region below 10 MHz increases with increasing Li substitution,  $x$ . Permeability is related to  $M_s$  and to the anisotropy constant and both parameters are modified with Li inclusion (Table 1).

As  $x$  is increased, the natural resonance frequency (the value where the imaginary permeability has a maximum value) shifts towards a lower frequency (from 52 to 17 MHz). The imaginary permeability in the low-frequency region below 100MHz is increased with an increase in  $x$ .

It is well accepted that there are two mechanisms responsible for the profiles of permeability spectra: domain-wall movement and spin rotation.

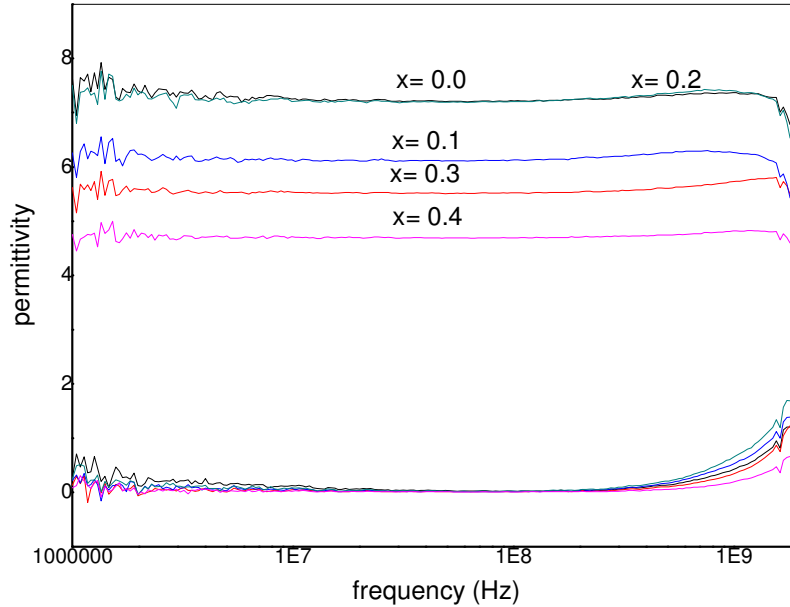


**Figure 5.** Real and imaginary permittivity ( $\epsilon'$  and  $\epsilon''$ ) of the studied samples in the 1MHz-1.8GHz range.

Dielectric properties of the ferrite samples are influenced by various factors: method of preparation, sintering conditions, chemical composition, ionic charge, grain size, etc. The microwave permittivity spectra ( $\epsilon'$ ) of these samples (Figure 5) indicate that the real parts do not change with frequency in the studied range. The  $\epsilon'$  values decrease from 7.2 to 4.6 for  $x=0$  to  $x=0.4$ . There are two mechanisms responsible for the permittivity dispersion: electron polarization and ion polarization. Novikova [11] has pointed out that there is a strong correlation between the conduction mechanism (hopping) and the dielectric behavior of ferrites. By electronic exchange,  $\text{Fe}^{3+} \rightarrow \text{Fe}^{2+}$  and  $\text{Mn}^{2+} \rightarrow \text{Mn}^{3+}$ , local electrons displacements determine the polarization of the ferrites. Li inclusion modifies the original  $\text{Fe}^{3+}/\text{Mn}^{2+}$  ratio (refer to the stoichiometric formula) so permittivity decreases while resistivity slightly increases from  $2.1 \times 10^{-7} \Omega\text{cm}$  to  $4.4 \times 10^{-7} \Omega\text{cm}$  for  $x=0$  to  $x=0.4$ , respectively.

Resistivity and the dielectric constant are important parameters when considering ferrites from the application point of view.

The variation of DC resistivity (at room temperature) and the dielectric constant (at 1 MHz frequency) with Li content is shown in Figure 6. It is clear from the figure that  $\log \rho$  and  $\epsilon'$  show inverse variation trends with each other due to their inverse interdependence. Since the dielectric constant is inversely proportional to the square root of resistivity, such a variation is not unexpected. The sample with  $x=0.4$  has maximum resistivity ( $4.4 \times 10^7 \Omega\text{cm}$ ) and minimum dielectric constant (4.65). As both the dielectric constant and the electrical conductivity are basically transport properties, their variation with composition is similar.

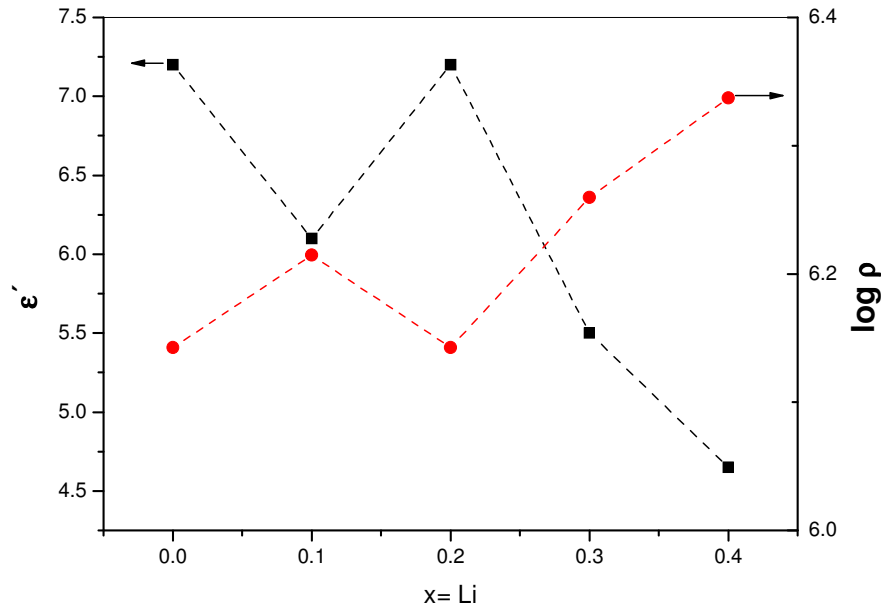


**Figure 6.** Compositional variation of DC electrical resistivity ( $\log \rho$  ( $\Omega$  cm)) and dielectric constant ( $\epsilon'$  at 1MHz) of  $\text{Li}_{0.5x}\text{Mn}_{0.4}\text{Zn}_{0.6-x}\text{Fe}_{2+0.5x}\text{O}_4$ .

It is clear from Figure 6 that the substitution of Li at a tetrahedral site (for Fe), results in an increase of resistivity for this kind of ferrites.

Permittivity losses profiles ( $\epsilon''$ ) show that resonant phenomena occur at frequencies higher than 1.9 GHz.

Electromagnetic wave absorption (reflection loss) was also studied using polycrystalline Li-Mn-Zn ferrite. Ferrite sintered ceramics have been used as very thin and extremely wide band electromagnetic wave absorbers in VHF and UHF bands [12]. The wide band characteristics are achieved by the frequency dispersion of the complex permeability: the imaginary part of the permeability ( $\mu''$ ) is almost inversely proportional to the frequency in these frequency bands. That is, the spin rotational relaxation component plays an important role in determining the absorption band.

In this frequency range the reflection loss ( $R_L$ ) is calculated as

$$R_L (dB) = 20 \log \left| \frac{Z_{in} - 1}{Z_{in} + 1} \right|, \quad (1)$$

where  $Z_{in}$  is the normalized input impedance in free space

$$Z_{in} = \sqrt{\mu_r / \epsilon_r} \tanh \left[ -i(2\pi / c) (\sqrt{\mu_r \epsilon_r}) f d \right] \quad (2)$$

where  $\mu_r$  and  $\epsilon_r$  are the relative complex permeability and permittivity of the absorber medium,  $f$  and  $c$  are, respectively, the frequency of microwave in free space and the velocity of light,  $d$  is the sample thickness [13]. Using the experimental values of the complex permeability and permittivity (equations 1 and 2), it is possible to estimate the absorption properties.

The electromagnetic wave absorption characteristics of polycrystalline Li-Mn-Zn ferrite are shown in Figure 7 and Table 2. The samples exhibit the potential of relatively wide band absorption in the frequency region from 140 MHz to 1.8 GHz. The center frequency shifts to lower values as  $x$  is increased and it can be tunable in the range from 150 to 304 MHz. For having an absorption

greater than 20dB (> 99 % absorption) these ferrites can be used as EMI shielding between 10 to 40 MHz.

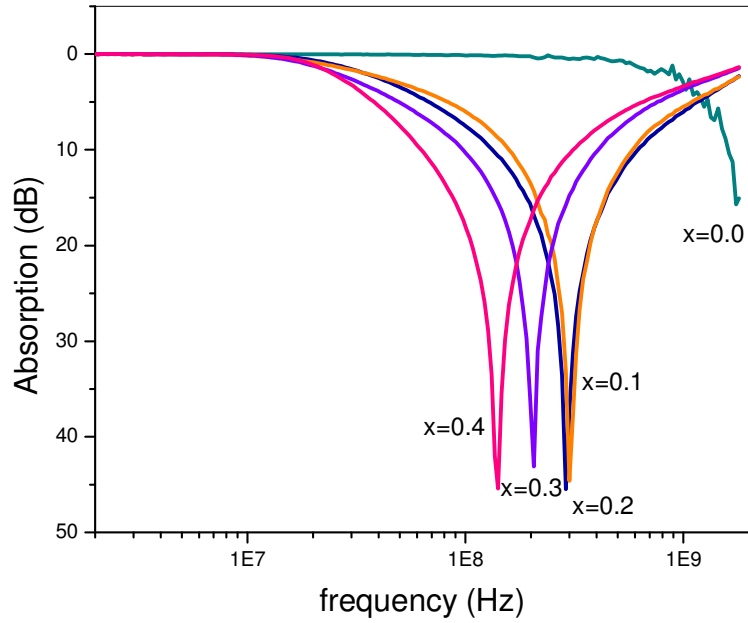


**Figure 7.** Calculated absorption spectra of  $\text{Li}_{0.5x}\text{Mn}_{0.4}\text{Zn}_{0.6-x}\text{Fe}_{2+0.5x}\text{O}_4$ .

All the substituted samples exhibit the potential of relative wide band absorption (100Hz). Values as high as 45 dB are obtained with Li substitution (Figure 7).

Table 2: Center frequency and absorption band for the polycrystalline Li–Mn–Zn ferrite single-layered absorbers.

Li content (x)	Center frequency [MHz]	Bandwidth (>20dB) [MHz]
0.0	1800	-
0.1	304	142
0.2	295	121
0.3	206	89
0.4	140	80

#### 4. Conclusions

Li-doped MnZn ferrites were successfully prepared by the ceramic method. XRD confirms the spinel phase for all compositions. Saturation magnetization increases with Li substitution. Lithium inclusion enhances microwave properties as it plays an important role in changing the structural and magnetic properties of these MnZn ferrites. As the Li content is increased, the low-frequency permeability increases and the natural resonance frequency shifts to lower values. The sample with higher Li content ( $x=0.4$ ) has maximum resistivity ( $4.4 \times 10^7 \Omega \text{ cm}$ ) and minimum dielectric constant (4.65).

The spin rotation component plays an important role in the high-frequency region. All the substituted samples exhibit the potential of relative wide band absorption (100Hz). Lithium inclusion enhances microwave absorption with a maximum reflection loss of 45 dB at 140M Hz for  $x=0.4$ . These characteristics suggest that high-frequency devices such as single-layered electromagnetic wave absorbers can be designed using these polycrystalline Li-Mn-Zn ferrites.

### Acknowledgements

This work was partially funded by UBACyT, Secyt-UNC and Conicet.

### References

- [1] J. Qiu, L. Lan, H. Zhang, M. Gu, J. All. Comp. 453 (2008) 261.
- [2] P. P. Hankare, R. P. Patil, U. B. Sankpal, S. D.J adhav, I. S. Mulla, K. M. Jadhav, B. K. Chougule, J. Mag. Magn. Mater. 321 (2009) 3270.
- [3] G.Ott, J.Wrba, R. Lucke, J. Magn. Magn. Mater. 535 (2003) 254–255.
- [4] U. Ghazanfar, S. A. Siddiqi, G. Abbas, Mater. Sci. Eng. B 118 (2005) 84.
- [5] S. Sugimoto, K. Haga, T. Kagotani, K. Inomata, J. Magn. Mag. Mat. 290-291 (2005) 1188.
- [6] T. Nakamura, T. Miyamoto, Y. Yamadaet, Journal of Magnetism and Magnetic Materials 256 (2003) 340–347.
- [7] J. Smit, H. Wijn, “Ferrites” . Philips’ Technical Library (1958).
- [8] C. Sun, K. Sun, Phys. B 391 (2007) 335.
- [9] H. Demidzu, T.Nakamura, Y.Yamada, J. Magn. Magn. Mater. 322-13 (2010) 1816-1821. Doi: 10.1016/j.jmmm.2009.12.033.
- [10] H. Shokrollahi, J. Magn. Magn. Mater. 320 (2008) 463.
- [11] L. I. Rabkin, Z. I. Novikova, Ferrotos, Izs. Acad. Nauk. BSSR. Minsk (1960) 146.
- [12] Y. Naito, K. Suetake, IEEE Trans. Microwave Theory Tech. 19 (1971) 65.
- [13] S. M. Abbas, A. K. Dixit, R. Chatterjee and T.C. Goel, J. Magn. Magn. Mater. 309 (2007) 20.